



University of Vaasa  
VAASAN YLIOPISTO

OSUVA Open  
Science

This is a self-archived – parallel published version of this article in the publication archive of the University of Vaasa. It might differ from the original.

## MODWT-Based Wavelet Neuro-Fuzzy MPPT for Photovoltaic Systems with Comparative Analysis to Machine Learning Controllers

Author(s): Kamal, Tariq; Hassan, Syed Zulqadar

Title: MODWT-Based Wavelet Neuro-Fuzzy MPPT for Photovoltaic Systems with Comparative Analysis to Machine Learning Controllers

Year: 2026

Version: Accepted manuscript

Copyright ©2026 IEEE. Personal use of this material is permitted. Permission from IEEE must be obtained for all other uses, in any current or future media, including reprinting/republishing this material for advertising or promotional purposes, creating new collective works, for resale or redistribution to servers or lists, or reuse of any copyrighted component of this work in other works.

Please cite the original version:

Kamal, T. & Hassan, S. Z. (2026). MODWT-Based Wavelet Neuro-Fuzzy MPPT for Photovoltaic Systems with Comparative Analysis to Machine Learning Controllers. *2026 International Conference on Data Science, Machine Learning, and Intelligence (DataSciMI)*.  
<https://doi.org/10.1109/DataSciMI67380.2026.11524011>

# MODWT-Based Wavelet Neuro-Fuzzy MPPT for Photovoltaic Systems with Comparative Analysis to Machine Learning Controllers

Tariq Kamal<sup>1,2</sup>, Syed Zulqadar Hassan<sup>\*3</sup>

<sup>1</sup>*School of Technology and Innovations, Electrical Engineering, University of Vaasa, Vaasa, Finland*

<sup>2</sup>*Arcada University of Applied Sciences, Jan-Magnus Janssons Plats 1, Helsinki, Finland*

<sup>3</sup>*Department of Computer Science, Faculty of IT & CS, University of Central Punjab, Lahore, Pakistan*  
tariq.kamal@uwasa.fi, zulqadar.hassan@ucp.edu.pk

**Abstract**—Accurate maximum power point tracking (MPPT) is critical for photovoltaic (PV) systems because the optimal operating point shifts continuously with irradiance and cell temperature. This paper studies a predictive MPPT strategy that combines (i) shift-invariant, multi-resolution features extracted from irradiance/temperature time series using the maximal overlap discrete wavelet transform (MODWT) with a Daubechies-4 (db4) mother wavelet and a three-level decomposition and (ii) a first-order Takagi-Sugeno neuro-fuzzy model that maps those features to a reference MPP voltage. The proposed wavelet neuro-fuzzy (WNF) controller is benchmarked against four common regression baselines (decision tree, random forest, support vector regression, and a multilayer perceptron ANN) using 48 h of per-minute weather data for Lahore, Pakistan (22–23 June 2025). In a 100 kW PV boost-converter simulation, the WNF controller achieves 99.988% average tracking efficiency and yields 1533.7 kWh, which is approximately 2% higher energy than the compared learning baselines under the same test conditions. We also discuss computational implications of MODWT-based feature extraction for real-time embedded MPPT.

**Keywords**—Maximum Power Point Tracking, Photovoltaic Systems, Wavelet Neuro-Fuzzy, Artificial Intelligence, Machine Learning, Renewable Energy Control

## I. INTRODUCTION

The accelerating deployment of photovoltaic (PV) systems is essential to global efforts in decarbonization and grid modernization. Due to continuous enhancements in PV module efficiency and reductions in manufacturing costs, PV has become increasingly competitive with conventional power sources. However, the output power of a PV array is highly sensitive to environmental settings especially solar irradiance and cell temperature and exhibits nonlinear current–voltage (I–V) and power–voltage (P–V) curves. Thus, maintaining operation at the Maximum Power Point (MPP) is essential to maximize energy harvesting under dynamic conditions.

Traditional MPPT methods, such as Perturb and Observe and Incremental Conductance have been widely used because of their simplicity and low computational demand. However, several limitations are observed in practice. Persistent oscillations around the maximum power point often occur especially under steady conditions. During rapid irradiance variations the response is usually slow. In cases of partial shading where multiple local peaks appear in the power voltage curve the global maximum power point cannot always be identified reliably [1], [2]. As reported in many review studies, these weaknesses lead to reduced energy yield particularly under real operating conditions [3].

In order to address these issues, increasing attention has been given to intelligent and data driven MPPT approaches. Advanced techniques such as fuzzy logic systems, artificial

neural networks, hybrid neuro fuzzy structures and wavelet based signal processing have been introduced. Through these methods, the optimal operating point is estimated from measured environmental and system inputs, allowing more accurate and adaptive control of photovoltaic systems [4], [5]. For instance, in [6], the authors proposed a neuro-fuzzy indirect wavelet-based adaptive MPPT controller combining wavelet transform, fuzzy reasoning, and neural network learning, demonstrating improved convergence speed and efficiency compared to conventional methods. Adaptive neuro-fuzzy feedback-linearization controllers have also been studied to handle PV nonlinearity and environmental uncertainties [7]. Moreover, in many studies adaptive neuro-fuzzy feedback-linearization controllers have also been studied to handle PV nonlinearity and environmental uncertainties [8], [9], [10], [11].

To date, many existing intelligent control strategies either lack feature engineering specifically designed to capture temporal dynamics or fail to effectively integrate multi-resolution signal analysis with data-driven learning models. In particular, using wavelet-based predictive features in conjunction with neuro-fuzzy systems offers potential advantages by taking both short-term fluctuations and trends in environmental variables. However, a comprehensive comparative evaluation of such a wavelet neuro-fuzzy architecture against state-of-the-art machine learning alternatives under realistic PV conditions is still open for contribution.

In this paper, we present a WNF MPPT controller that combines maximal overlap discrete wavelet transform using predictive feature extraction with a Takagi–Sugeno neuro-fuzzy inference system for dynamic adaptability. We tested this WNF controller against four representative machine learning models Decision Tree, Random Forest, Support Vector Regression (SVR), and Artificial Neural Network (ANN) using simulation scenarios with varying irradiance, temperature, and partial shading conditions. Our results show that the WNF architecture attains better tracking precision, faster transient response and 2% higher total energy yield than benchmarks, validating the efficacy of predictive feature integration in intelligent MPPT design.

The rest of the paper is organized as follows: Section II describes the PV system and converter modeling. Section III details the design of MPPT controllers, including the proposed WNF. Section IV defines performance metrics and simulation protocol. Section V presents and discusses comparative results. Final section offers conclusion and future work.

## II. PHOTOVOLTAIC SYSTEM MODELING

An accurate model of the PV system is essential for designing and testing any MPPT controller. In this work, the

PV array was represented using the single-diode, five-parameter model, which provides a good balance of accuracy and computational simplicity [12], [13]. This model's current-voltage (I-V) characteristic is described by the following equation:

$$I = I_{ph}(G, T_c) - I_0(T_c) - \frac{V + IR_s}{R_{sh}} \quad (1)$$

The five parameters defining the model are the photocurrent ( $I_{ph}$ ), the diode reverse saturation current ( $I_0$ ), the diode ideality factor ( $\alpha$ ), the series resistance ( $R_s$ ), and the shunt resistance ( $R_{sh}$ ). The accuracy of this model is highly dependent on the correct identification of these parameters, a process known as parameter extraction [14], [15].

The model must also account for the influence of environmental conditions, specifically solar irradiance ( $G$ ) and cell temperature ( $T_c$ ). This is primarily achieved by adjusting the photocurrent and reverse saturation current. The photocurrent is nearly proportional to irradiance, while the saturation current has a strong exponential dependence on temperature. These relationships are expressed as:

$$I_{ph}(G, T_c) = \left( \frac{G}{G_{ref}} \right) \quad (2)$$

$$I_0(T_c) = I_{0,ref} \left( \frac{T_c}{T_{ref}} \right)^3 \exp \left[ -\frac{E_g}{nk} \left( \frac{1}{T_c} - \frac{1}{T_{ref}} \right) \right] \quad (3)$$

Here, the 'ref' subscript indicates values at standard test conditions,  $E_g$  is the semiconductor bandgap energy. These equations capture the fundamental behavior of the PV array under varying weather.

The MPPT algorithm determines the target operating voltage, but a power electronics interface is needed to apply it to the PV array. A DC-DC boost converter is used for this purpose. The converter's duty cycle ( $d$ ) is adjusted to change the effective impedance seen by the array, thereby controlling its operating voltage. Initially, discrete Proportional-Integral (PI) controller is used to manage this process, which is later on replaced with other controllers. The controller calculates the error between the MPPT's reference voltage ( $V_{ref}$ ) and the measured PV voltage ( $V_{pv}$ ) and adjusts the duty cycle accordingly to minimize this error. The control action is described by:

$$e_v[n] = V_{ref}[n] - V_{pv}[n] \quad (4)$$

$$d[n] = \text{sat} \left( d[n-1] + K_p e_v[n] + K_i \sum_{k=0}^n e_v[k] \Delta t \right) \quad (5)$$

This inner control loop must be fast and stable to accurately follow the commands from the main MPPT controller [16], [17].

### III. INTELLIGENT CONTROLLER ARCHITECTURES

A key limitation of many MPPT controllers is that they are reactive, meaning they only respond to a change after it has occurred. For superior performance in dynamic conditions, a controller needs predictive capabilities. This can be achieved by providing it with features that describe not just the current state but also the trends and rates of change in the environment. The Maximal-Overlap Discrete Wavelet Transform is a signal processing tool used here for this

purpose. It decomposes the time-series data of irradiance and temperature into components at different frequency scales [16], [18]. This multi-resolution analysis provides a rich set of features that capture both short-term fluctuations and long-term trends, which are then used as inputs for the intelligent controllers.

In this study, the MODWT is implemented using the Daubechies-4 (db4) mother wavelet with a three-level decomposition ( $J = 3$ ), consistent with the feature extraction used in the accompanying source implementation. For an input sequence  $x_t$  of length  $N$ , the MODWT detail and scaling coefficients at level  $j$  are computed via circular convolution with the rescaled wavelet and scaling filters  $\tilde{h}_{j,l}$  and  $\tilde{g}_{j,l}$  [16], [18]:

$$W_{j,t} = \sum_{l=0}^{L-1} \tilde{h}_{j,l} x_{(t-l) \bmod N} \quad (6)$$

$$V_{j,t} = \sum_{l=0}^{L-1} \tilde{g}_{j,l} x_{(t-l) \bmod N} \quad (7)$$

where  $L$  is the filter length determined by the selected mother wavelet (here, db4).

The primary controller analyzed in this study is a Wavelet Neuro-Fuzzy model. This is a hybrid architecture that combines a neuro-fuzzy inference system with the feature set generated by the MODWT [4], [17], [19]. The core of the WNF is a five-layer network that implements a first-order Takagi-Sugeno fuzzy model is shown in figure 1. The input layer receives the feature vector from the MODWT. The second layer, or fuzzification layer, calculates the degree of membership of each input feature to various fuzzy sets using Gaussian membership functions:

$$\mu_{r,i}(z_i) = \exp \left( -\frac{(z_i - c_{r,i})^2}{2\sigma_{r,i}^2} \right) \quad (8)$$

The parameters  $c_{r,i}$  and  $\sigma_{r,i}$  define the center and width of these functions and are learned during training. The third layer of the WNF model is the rule layer, where the firing strength of each fuzzy rule is calculated. This is done by multiplying the membership values from the previous layer:

$$\omega_r = \prod_i \mu_{r,i}(z_i) \quad (9)$$

The fourth layer normalizes these firing strengths and computes the output of each rule's consequent. In the Takagi-Sugeno model, the consequent is a linear function of the inputs:

$$\bar{\omega}_r = \frac{\omega_r}{\sum_{q=1}^R \omega_q} \quad (10)$$

$$y_r = \mathbf{a}_r^T \mathbf{z} + b_r = \sum_i a_{r,i} z_i + b_r \quad (11)$$

The final output of the WNF controller is computed in the fifth layer, which is a single node that calculates the weighted average of all rule consequents. This provides the final reference voltage,  $\hat{V}_{ref}$ .

$$\hat{V}_{ref} = \sum_{r=1}^R \bar{\omega}_r y_r \quad (12)$$

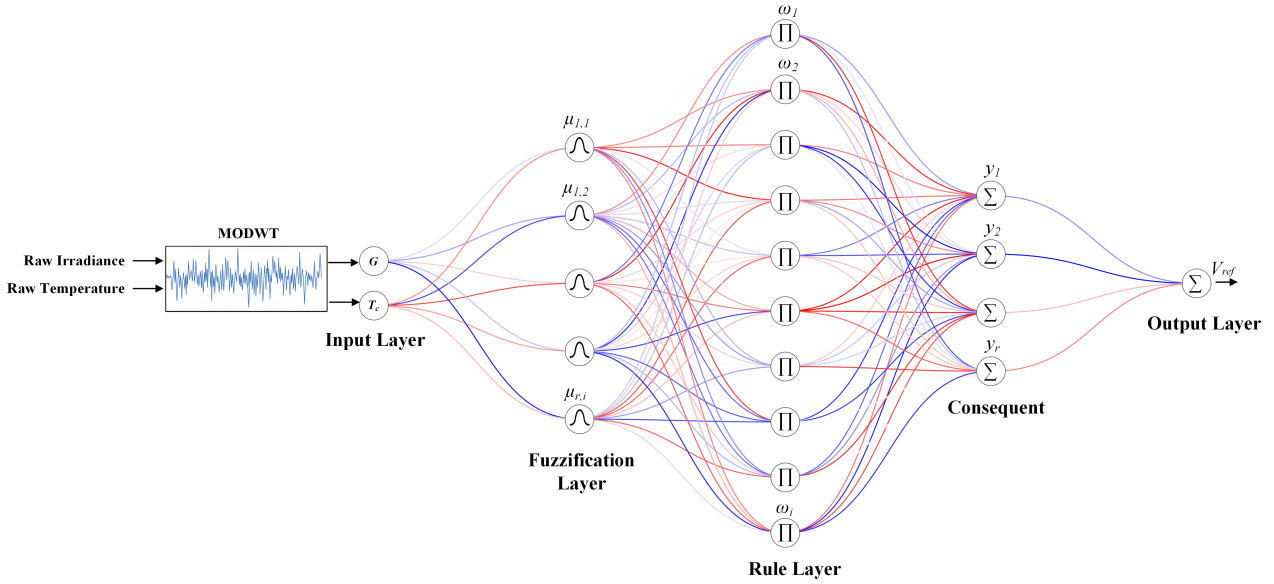


Fig. 1. Five-layer model of ANF featured with MODWT

This structure allows the WNF controller to learn a complex, non-linear, and dynamic mapping from the environmental trends to the optimal operating voltage, enabling it to anticipate changes in the MPP.

To assess the performance of the WNF controller, a comparison was carried out with four well-known machine learning models. First, a Decision Tree model was considered. In this approach, the input space is divided into smaller regions based on a set of hierarchical rules. For each region, the prediction is determined from the average value of the training samples that fall within that partition [20], [21]. A Random Forest model was also examined. In this method, several decision trees are built instead of using a single tree. The final output is obtained by averaging the results of all trees, which improves stability and reduces overfitting [22], [23].

Support Vector Regression was selected as the third benchmark. Here, a function is determined so that errors remain within a defined margin while keeping the model smooth. Nonlinear relationships are handled through kernel functions, allowing complex data patterns to be captured effectively [24].

In addition, a Multi-Layer Perceptron with two hidden layers was used as a standard Artificial Neural Network model. This structure is widely applied in regression problems due to its ability to learn nonlinear relationships between inputs and outputs [4], [25], [26], [27]. Together, these models provide a balanced reference for evaluating the proposed WNF architecture.

#### IV. PERFORMANCE METRICS

Controller performance is evaluated using both instantaneous tracking behavior and aggregated indices computed from the power tracking error  $e_p[n] = P_{ref}[n] - P[n]$ . The primary metric reported is the *average tracking efficiency*, defined as the ratio of harvested energy to available maximum energy over the simulation horizon:

$$\bar{\eta} = \frac{\sum_n P[n]\Delta t}{\sum_n P_{ref}[n]\Delta t} \quad (13)$$

In addition, we report error-based metrics (RMSE and MAE) and cumulative energy yield, as commonly used in MPPT evaluations [3], [13].

#### V. RESULTS AND DISCUSSION

The real-time irradiance and temperature data were obtained from the Copernicus Atmosphere Monitoring Service [28] and WeatherBit Historical Weather (per-minute intervals) [29] for Lahore, Pakistan, located at latitude 31.5204°N and longitude 74.3587°E. The dataset used for testing covers the period from 22 June 2025 to 23 June 2025.

Five MPPT algorithms were evaluated on a simulated 100 kW solar array: Decision Tree (Tree), Random Forest (RF), Support Vector Machine (SVM), Artificial Neural Network (ANN), and Wavelet Neuro-Fuzzy (WNF). The test was run for 48 hours using real weather data. The real time irradiance and temperature used for testing is shown in figure 2.

##### A. Controller Performance Under Normal Operation

For a comparison, all the controller are trained separately. This setup allowed a clear comparison in both steady and changing weather. Figure 3 shows how each controller tracked the reference maximum power ( $P_{Ref}$ ). All controllers tracked reasonably well, but clear gaps appeared during rapid weather changes. Figure 4 shows the operating voltage relative to the true  $V_{mp}$ .

##### B. Dynamic Response Analysis

Two intervals with abrupt irradiance changes, from 595 to 600 min and from 2195 to 2205 min, are highlighted in figure 5. In both cases, the WNF controller shows a smaller transient power error. This is in line with its design. The MODWT features capture both short term variations and longer trends, allowing the neuro fuzzy model to respond more effectively to rapid changes.

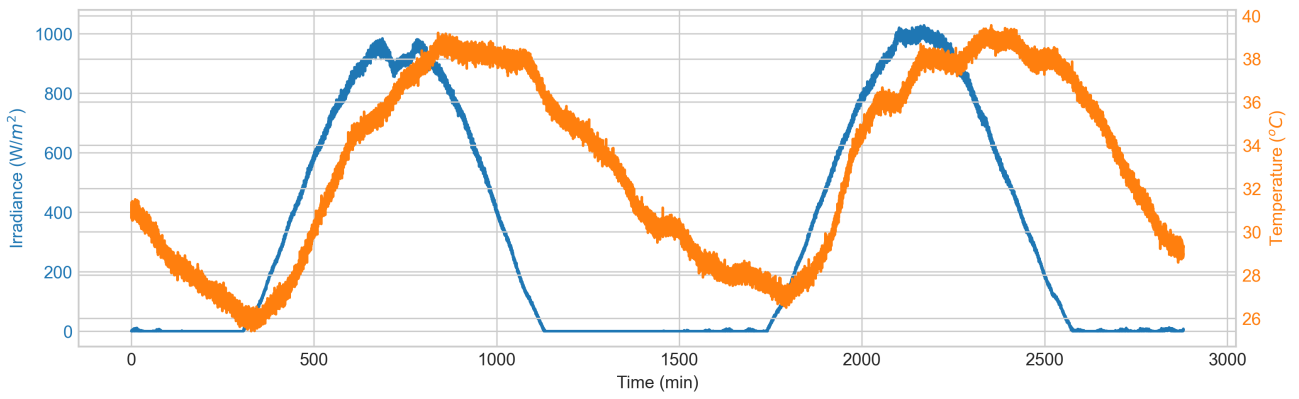


Fig. 2. Irradiance and temperature inputs over the simulation period

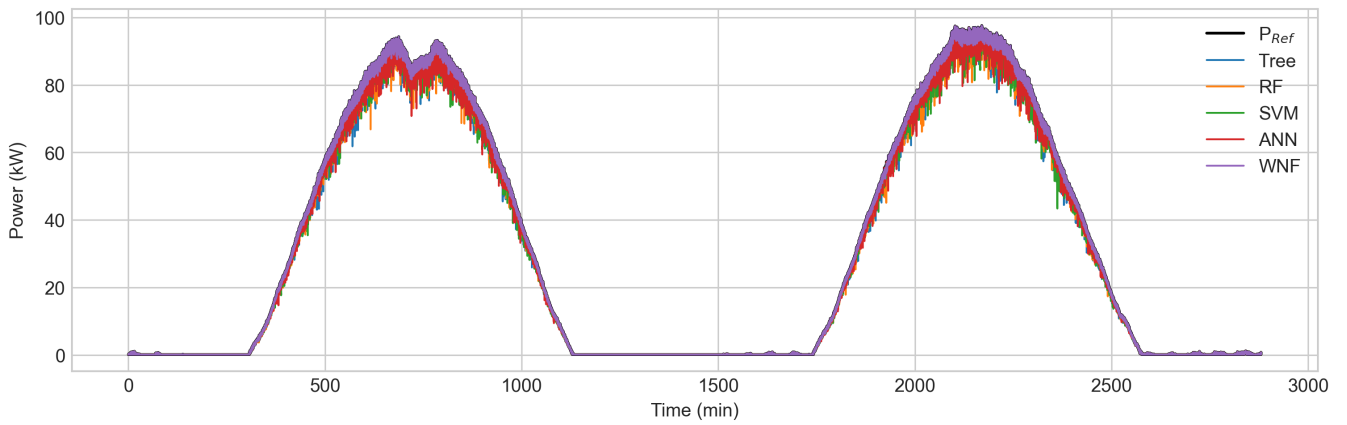


Fig. 3. Overall PV power tracking for all controllers versus the reference power ( $P_{Ref}$ ).

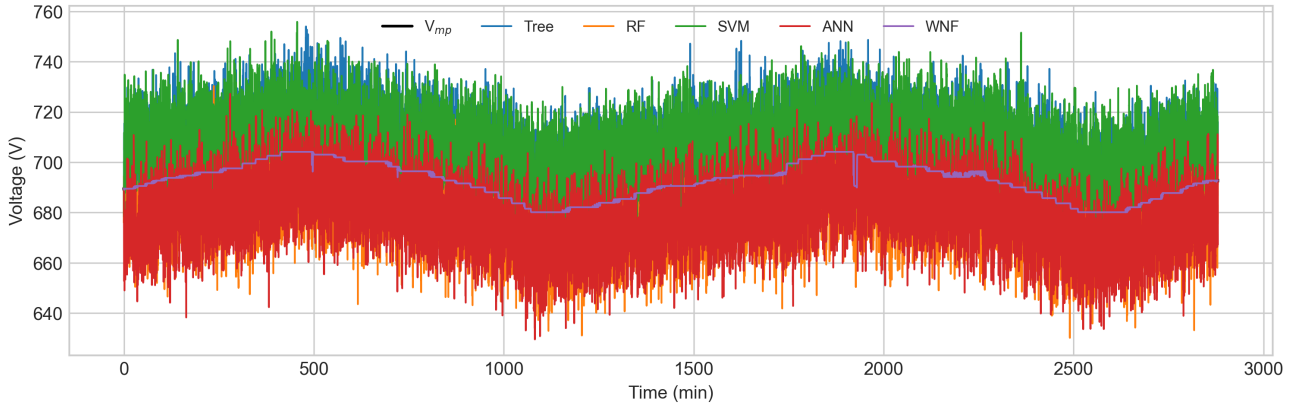


Fig. 4. Operating voltage tracking versus the true  $V_{mp}$  for each controller

### Zoomed-In Power Tracking at Key Intervals

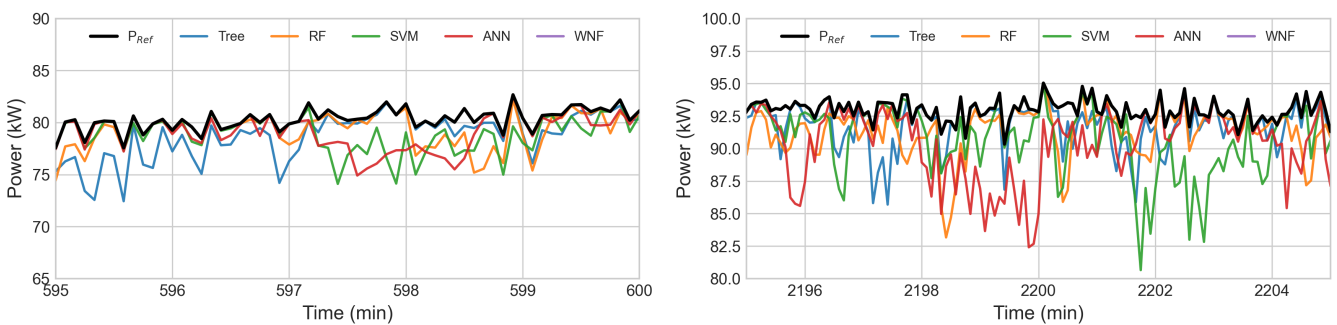


Fig. 5. Zoomed-in power tracking during two dynamic intervals

Figure 6 shows the instantaneous and average efficiency over time. The WNF controller remains close to 100% across the full profile, while the other regression methods show clear efficiency drops during transient events.

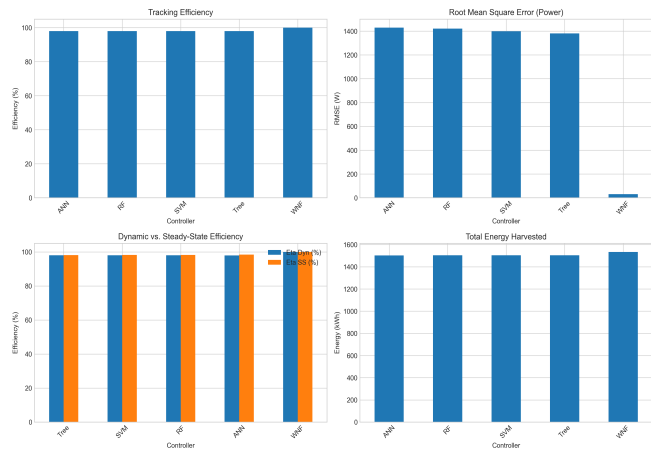


Fig. 6. Instantaneous (solid) and average (dashed) tracking efficiency over time.

### C. Quantitative Performance Metrics

Table I presents the main performance metrics. The proposed WNF controller reaches an average efficiency of 99.98% and delivers 1533.7 kWh. In contrast, the other learning based methods stay around 98% efficiency, with an energy output close to 1503 kWh.

TABLE I. PERFORMANCE SUMMARY OF MPPT CONTROLLERS

Controller	$\eta$ (%)	RMSE (W)	Energy (kW)	MAE (kW)
Tree	98.02	1380.2	1503.6	0.630
RF	98.01	1420.4	1503.2	0.639
SVM	98.02	1398.6	1503.5	0.631
ANN	97.97	1428.4	1502.7	0.649
WNF	99.98	31.27	1533.6	0.004

Figure 7 shows the running RMSE and cumulative energy curves. The WNF controller keeps the tracking error low during the entire simulation. Over 48 h, this leads to a clear gain in total energy.

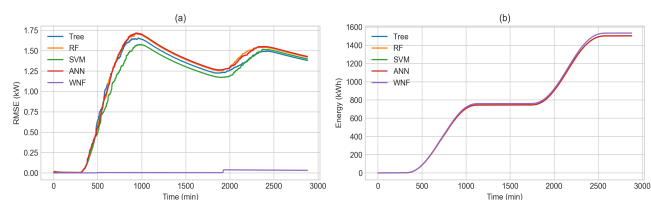


Fig. 7. Running metrics: (a) RMSE of power tracking (b) cumulative energy harvested

Figure 8 compares the cumulative error indices, including IAE, ITAE, ISE, and ITSE. The results confirm that the WNF approach reduces both the size of the errors and how long they persist.

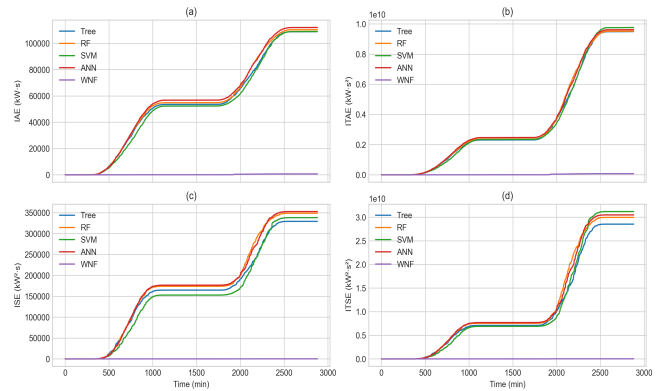


Fig. 8. Running integrated error indices: (a) IAE, (b) ITAE, (c) ISE, and (d) ITSE.

### CONCLUSION

In this work, several data driven MPPT controllers for photovoltaic systems were examined with particular emphasis placed on the WNF structure. By combining MODWT based feature extraction with an adaptive Takagi Sugeno fuzzy inference system, high tracking accuracy was achieved and stable operation was maintained during rapid irradiance variations. The efficiency was kept close to 99.98%, and nearly 2% more total energy was obtained compared to Decision Tree, Random Forest, SVR, and ANN models. These results show that when multi resolution environmental features are included, the controller response to changing conditions is clearly improved.

The proposed WNF approach can be considered a reliable foundation for advanced MPPT strategies in large scale and grid connected PV systems. Further validation through hardware in the loop testing and real time embedded implementation is planned. In addition, reinforcement learning methods may be incorporated to support more adaptive and self-optimizing photovoltaic control in future developments.

### REFERENCES

- [1] L. Bhukya, N. R. Kedika, and S. R. Salkuti, "Enhanced Maximum Power Point Techniques for Solar Photovoltaic System under Uniform Insolation and Partial Shading Conditions: A Review," *Algorithms*, vol. 15, no. 10, 2022, doi: 10.3390/a15100365.
- [2] R. I. Jabbar, S. Mekhilef, M. Mubin, O. Alshammari, and A. Kazaili, "A Fast MPPT Method Based on Improved Water Cycle Optimization Algorithm for Photovoltaic Systems Under Partial Shading Conditions and Load Variations," *IEEE Open Journal of the Industrial Electronics Society*, vol. 5, pp. 1324–1338, 2024, doi: 10.1109/OJIES.2024.3510367.
- [3] M. Sarvi and A. Azadian, "A comprehensive review and classified comparison of MPPT algorithms in PV systems," *Energy Systems*, vol. 13, no. 2, pp. 281–320, 2022.
- [4] S. Danyali, M. Babaeifard, M. Shirkhani, A. Azizi, J. Tavoosi, and Z. Davdand, "A new neuro-fuzzy controller based maximum power point tracking for a partially shaded grid-connected photovoltaic system," *Heliyon*, vol. 10, no. 17, p. e36747, 2024, doi: https://doi.org/10.1016/j.heliyon.2024.e36747.
- [5] S. Farajdadian and S. M. H. Hosseini, "DMPPT control of photovoltaic systems under partial shading conditions based on optimized neural networks," *Soft comput.*, vol. 28, no. 6, pp. 4987–5014, 2024, doi: 10.1007/s00500-023-09196-4.
- [6] S. Z. Hassan, H. Li, T. Kamal, U. Arifoğlu, S. Mumtaz, and L. Khan, "Neuro-Fuzzy Wavelet Based Adaptive MPPT Algorithm for Photovoltaic Systems," *Energies (Basel)*, vol. 10, no. 3, 2017, doi: 10.3390/en10030394.

- [7] M. Awais, L. Khan, S. Ahmad, S. Mumtaz, and R. Badar, "Nonlinear adaptive NeuroFuzzy feedback linearization based MPPT control schemes for photovoltaic system in microgrid," *PLoS One*, vol. 15, no. 6, p. e0234992, Jun. 2020, doi: 10.1371/journal.pone.0234992.
- [8] S. Mumtaz, S. Ahmad, L. Khan, S. Ali, T. Kamal, and S. Z. Hassan, "Adaptive Feedback Linearization Based NeuroFuzzy Maximum Power Point Tracking for a Photovoltaic System," *Energies (Basel)*, vol. 11, no. 3, 2018, doi: 10.3390/en11030606.
- [9] S. Z. Hassan, H. Li, T. Kamal, M. Nadarajah, and F. Mehmood, "Fuzzy embedded MPPT modeling and control of PV system in a hybrid power system," in *2016 International Conference on Emerging Technologies (ICET)*, 2016, pp. 1–6. doi: 10.1109/ICET.2016.7813236.
- [10] M. E. Girgis and N. A. Elkhateeb, "Enhancing photovoltaic MPPT with P&O algorithm performance based on adaptive PID control using exponential forgetting recursive least squares method," *Renew. Energy*, vol. 237, p. 121801, 2024, doi: <https://doi.org/10.1016/j.renene.2024.121801>.
- [11] C. Aoughlis, A. Belkaid, I. Colak, O. Guenounou, and M. A. Kacimi, "Automatic and Self Adaptive P&O MPPT Based PID Controller and PSO Algorithm," in *2021 10th International Conference on Renewable Energy Research and Application (ICRERA)*, 2021, pp. 385–390. doi: 10.1109/ICRERA52334.2021.9598489.
- [12] X. Hao, P. Liu, Y. Deng, and X. Meng, "A MIC-LSTM based parameter extraction method for single-diode PV model," *Front. Energy Res.*, vol. Volume 11-2023, 2024, doi: 10.3389/fenrg.2023.1349887.
- [13] A. Reza Reisi, M. Hassan Moradi, and S. Jamasb, "Classification and comparison of maximum power point tracking techniques for photovoltaic system: A review," *Renewable and Sustainable Energy Reviews*, vol. 19, pp. 433–443, 2013, doi: <https://doi.org/10.1016/j.rser.2012.11.052>.
- [14] R. Poley and A. Shirsavar, "Digital Peak Current Mode Control With Slope Compensation Using the TMS320F2803x," 2012.
- [15] Infineon Technologies AG, "Digital PFC CCM Boost Converter Using XMC1400 Microcontroller: 300-W Design Example," 2016.
- [16] P. Chaovalit, A. Gangopadhyay, G. Karabatis, and Z. Chen, "Discrete wavelet transform-based time series analysis and mining," *ACM Comput. Surv.*, vol. 43, no. 2, Feb. 2011, doi: 10.1145/1883612.1883613.
- [17] P. Biswal and A. K. Pati, "A Novel ANFIS Method for Detection of Maximum Power Point of Photovoltaic System," in *2023 International Conference on Communication, Circuits, and Systems (IC3S)*, 2023, pp. 1–6. doi: 10.1109/IC3S57698.2023.10169627.
- [18] S. Upadhyaya and A. Panda, "Implementation of MODWT on Real Time Power Quality Disturbance Signal," *International Journal of Innovative Technology and Exploring Engineering*, vol. 9, no. 5, pp. 796–800, Feb. 2020, doi: 10.35940/ijitee.E2484.039520.
- [19] Y. Türkay and A. G. Yükek, "Investigating the Potential of an ANFIS-Based Maximum Power Point Tracking Controller for Solar Photovoltaic Systems," *IEEE Access*, vol. 13, pp. 41768–41784, 2025, doi: 10.1109/ACCESS.2025.3547954.
- [20] P. V. Mahesh, S. Meyyappan, and R. R. Alla, "Maximum power point tracking using decision-tree machine-learning algorithm for photovoltaic systems," *Clean Energy*, vol. 6, no. 5, pp. 762–775, Feb. 2022, doi: 10.1093/ce/zkac057.
- [21] M. Bouksaim, M. Mekhfioui, and M. N. Srifi, "A Comprehensive Decade-Long Review of Advanced MPPT Algorithms for Enhanced Photovoltaic Efficiency," *Solar*, vol. 5, no. 3, 2025, doi: 10.3390/solar5030044.
- [22] A. Khalyasmaa *et al.*, "Prediction of Solar Power Generation Based on Random Forest Regressor Model," in *2019 International Multi-Conference on Engineering, Computer and Information Sciences (SIBIRCON)*, 2019, pp. 780–785. doi: 10.1109/SIBIRCON48586.2019.8958063.
- [23] M. A. Azman, H. Jantan, U. F. M. Bahrin, and E. A. Kadir, "Solar Power Production Forecasting Model Using Random Forest Algorithm," in *Intelligent Systems Design and Applications*, A. Abraham, A. Bajaj, T. Hanne, P. Siarry, and K. Ma, Eds., Cham: Springer Nature Switzerland, 2024, pp. 135–144. doi: 10.1007/978-3-031-64847-2\_12.
- [24] A. G. Abo-Khalil, "Maximum Power Point Tracking for a PV System Using Tuned Support Vector Regression by Particle Swarm Optimization," *Journal of Engineering Research*, vol. 8, no. 4, pp. 139–152, 2020, doi: <https://doi.org/10.36909/jer.v8i4.9113>.
- [25] A. Boudia, S. Messalti, S. Zeghlache, and A. Harrag, "Type-2 fuzzy logic controller-based maximum power point tracking for photovoltaic system," *Electrical Engineering & Electromechanics*, no. 1, pp. 16–22, Feb. 2025, doi: 10.20998/2074-272X.2025.1.03.
- [26] O. F. Kececioğlu, A. Gani, and M. Sekkeli, "Design and Hardware Implementation Based on Hybrid Structure for MPPT of PV System Using an Interval Type-2 TSK Fuzzy Logic Controller," *Energies (Basel)*, vol. 13, no. 7, 2020, doi: 10.3390/en13071842.
- [27] L. P. N. Jyothy and M. R. Sindhu, "An Artificial Neural Network based MPPT Algorithm For Solar PV System," in *2018 4th International Conference on Electrical Energy Systems (ICEES)*, 2018, pp. 375–380. doi: 10.1109/ICEES.2018.8443277.
- [28] Copernicus Atmosphere Monitoring Service, "CAMS solar radiation time-series," 2020. doi: 10.24381/5cab0912.
- [29] Weatherbit.io, "Weatherbit Historical Subhourly Weather Data API," 2025. Accessed: Sep. 01, 2025. [Online]. Available: <https://api.weatherbit.io/v2.0/history/subhourly?lat=31.5204&lon=74.3587&start date=2025-06-22&end date=2025-06-23&key=API KEY>